

# SPACE-CHARGE TRANSPORT LIMITS IN PERIODIC CHANNELS\*

Steven M. Lund, Lawrence Livermore National Laboratory, Livermore, CA 94550

Sugreev R. Chawla, Lawrence Berkeley National Laboratory, Berkeley, CA 94720

## Abstract

It has been empirically observed in both experiments and particle-in-cell simulations that space-charge-dominated beams suffer strong emittance growth and particle losses in alternating gradient quadrupole transport channels when the undepressed phase advance  $\sigma_0$  increases beyond about  $85^\circ$  per lattice period. Although this criteria has been used extensively in practical designs of intense beam transport lattices, no theory exists that explains the limit. We propose a mechanism for the transport limit resulting from classes of halo particle resonances near the core of the beam that allow near-edge particles to rapidly increase in oscillation amplitude when the space-charge intensity and the flutter of the matched beam envelope are both sufficiently large. Due to a finite beam edge and/or perturbations, this mechanism can result in dramatic halo-driven increases in statistical beam phase space area, lost particles, and degraded transport. A core-particle model for a uniform density elliptical beam in a periodic focusing lattice is applied to parametrically analyze this process.

## INTRODUCTION

The maximum transportable current of an ion beam with high space-charge intensity propagating in a periodic focusing lattice is a problem of practical importance[1]. Accelerator applications such as Heavy Ion Fusion (HIF), High Energy Density Physics (HEDP), and waste transmutation demand a large flux of particles on target. The maximum current can result from a variety of factors: instability of low-order moments of the beam describing the centroid and envelope, instability of higher order collective modes, statistical emittance growth, excessive halo generation, and species contamination associated with issues such as the electron cloud problem. Surprisingly, no theory exists to predict the current transportable in a periodic focusing lattice in the absence of focusing errors and species contamination (electron-cloud effects) beyond a moment level description of low-order beam instabilities. Moreover, although moment-based centroid and envelope descriptions reliably predict regions of parametric instability where machines cannot operate[2] such models appear to be overly optimistic when compared to simulations and experiments which observe degraded transport where the moment models predict stability[1].

Denote the phase advance of particles oscillating in a periodic focusing lattice in the presence and absence of beam space-charge by  $\sigma$  and  $\sigma_0$  (both measured in degrees per lattice period)[2, 3]. The undepressed phase-advance  $\sigma_0$  measures the strength of the linear applied focusing forces of the periodic lattice and is relatively insensitive to the details of the lattice.  $\sigma_0$  is made as large as beam stability will

allow – because stronger focusing results in smaller beam cross-sectional area leading to smaller, more economical accelerator structures. Conversely,  $\sigma$  is made as small as possible within injector limits for maximum current.

The depressed phase advance  $\sigma$  is defined by an rms equivalent, matched KV equilibrium beam[2, 3]. The ratio  $\sigma/\sigma_0$  is a normalized measure of relative space-charge strength with  $\sigma/\sigma_0 \rightarrow 1$  corresponding to a warm beam with zero space-charge forces and  $\sigma/\sigma_0 \rightarrow 0$  corresponding to a cold beam with the maximum possible current.

Neglecting image charge effects, single particle and beam centroid oscillations are stable if  $\sigma_0 < 180^\circ$ [2]. The parameter space  $\sigma_0 \in (0, 180^\circ)$  and  $\sigma/\sigma_0 \in (0, 1)$  can be regarded as potential operating points. Envelope models predict bands of strong parametric instability when  $\sigma_0 > 90^\circ$  and  $\sigma/\sigma_0 < 1$ . The extent of the parameter region excluded by the envelope band for FODO quadrupole transport is well understood[2] is indicated (in blue) on Fig. 1.

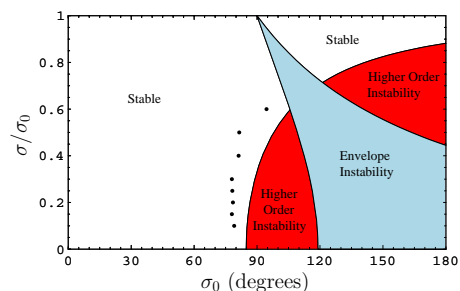


Figure 1: (Color) Beam stability regions in a FODO quadrupole lattice. Dots are core-particle model stability boundary points.

Considerations beyond centroid and envelope instabilities can exclude further regions of  $\sigma_0$ - $\sigma$  parameter space. Transportable current limits based on preservation of beam statistical emittance and suppression of particle losses for a matched beam propagating in a periodic channel of FODO electric quadrupoles were studied by Tiefenback at LBNL on the SBTE experiment[1]. It was found empirically that stable transport was obtained when

$$\sigma_0^2 - \sigma^2 < \frac{1}{2}(120^\circ)^2. \quad (1)$$

The parameter region this criteria excludes for machine operation (partially overlapping the envelope band) is indicated (in red) on Fig. 1. For high space-charge intensity with  $\sigma/\sigma_0 < 0.5$ , this limit is more important than the envelope stability limit because it is encountered first when approaching from low  $\sigma_0$ . The stability bound (1) has been applied by coarsely requiring that  $\sigma_0 < 120^\circ/\sqrt{2} \simeq 85^\circ$ . It is observed that transport becomes more sensitive to errors near the boundary of stability.

## PARTICLE-IN-CELL SIMULATIONS

Self-consistent particle-in-cell (PIC) simulations have been carried out for a variety of initial beam distributions launched in FODO quadrupole transport channels using

\* This research was performed at LLNL and LBNL under US DOE contact Nos. W-7405-Eng-48 and DE-AC03-76SF0098.

the WARP code[4]. Results are in qualitative agreement with Eq. (1). Parameters to the right of the stability bound but outside of the envelope stability band lead to statistical (rms) emittance growth and particle losses. Emittance growth can be rapid and large as illustrated in Fig. 2 for three distributions: an initial semi-Gaussian, waterbag “equilibrium”, and a thermal “equilibrium.” In all cases the initial distributions are rms matched (the “equilibrium” distributions are rms equivalent transformed from a continuous focusing equilibrium). The similarity of the results for the three very different non-equilibrium distributions shows that the transport limit is insensitive to the form of the initial distribution. Beams in real laboratory situations are born off a source (injector) and subsequently manipulated to match into a transport channel and are unlikely to be any equilibrium form.

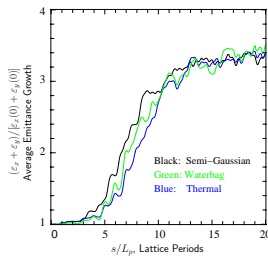


Figure 2: (Color) PIC simulations of emittance growth for different initial distributions in a FODO quadrupole channel. ( $\sigma_0 = 100^\circ$ ,  $\eta = 0.5$ ,  $L_p = 0.5$  m,  $\sigma/\sigma_0 = 0.2$ , and  $\varepsilon = 50$  mm-mrad).

### CORE-PARTICLE MODEL

We consider an unbunched beam of ions of charge  $q$  and mass  $m$  propagating with axial velocity  $\beta_b c$  ( $c$  is the speed of light *in vacuo*) and relativistic factor  $\gamma_b = 1/\sqrt{1 - \beta_b^2}$ . A linear applied focusing lattice is assumed, self-field interactions are electrostatic. Then the transverse orbit  $x(s)$  of a beam particle satisfy the paraxial equations of motion[2, 3]

$$x'' + \kappa_x x = -\frac{q}{m\gamma_b^3 \beta_b^2 c^2} \frac{\partial \phi}{\partial x}. \quad (2)$$

Here,  $s$  is the axial coordinate of a beam slice, primes denote derivatives with respect to  $s$ , and  $\kappa_x(s)$  is the linear applied focusing function of the lattice (specific forms can be found in Ref. [2]), and the electrostatic potential  $\phi$  is related to the number density of beam particles  $n$  by the Poisson equation  $\nabla_{\perp}^2 \phi = -qn/\epsilon_0$  in free-space.  $\epsilon_0$  is the permittivity of free space.

The core of the beam is centered on-axis ( $x = 0 = y$ ), and is uniform density within an elliptical cross-section with edge radii  $r_j$  (henceforth,  $j$  ranges over both  $x$  and  $y$ ) that obey the KV envelope equations

$$r_j'' + \kappa_j r_j - \frac{2Q}{r_x + r_y} - \frac{\varepsilon_j^2}{r_j^3} = 0. \quad (3)$$

Here,  $Q = q\lambda/(2\pi\epsilon_0 m\gamma_b^3 \beta_b^2 c^2) = \text{const}$  is the dimensionless perveance of the beam,  $\lambda = q\hat{n}r_x r_y = \text{const}$  ( $\hat{n}$  denotes the constant density within the beam envelope) is the line-charge density of the beam,  $\varepsilon_j$  is the statistical edge emittance of the beam along the  $j$ -plane. We take  $\varepsilon_j \equiv \varepsilon = \text{const}$ . When the beam is propagating in a periodic focusing channel with lattice period  $L_p$ ,  $\kappa_j(s + L_p) = \kappa_j(s)$ , the envelope is called matched when

it has the periodicity of the lattice,  $r_j(s + L_p) = r_j(s)$ . Undepressed particle phase advances are used to set the lattice focusing functions  $\kappa_j$  using  $\cos \sigma_0 = (1/2)\text{Tr}M$  where  $M$  is the  $x$  or  $y$  plane transfer map of a single particle ( $Q = 0$ ) through one lattice period. The depressed particle phase advance is calculated as  $\sigma = \varepsilon \int_0^{L_p} ds/r_j^2$ .

It can be shown that the flutter of the matched beam envelope for periodic FODO quadrupole focusing systems with piecewise constant  $\kappa_j(s)$  is given approximately by

$$\frac{r_x|_{\text{max}}}{\bar{r}_x} - 1 \simeq (1 - \cos \sigma_0)^{1/2} \frac{(1 - \eta/2)}{2^{3/2}(1 - 2\eta/3)^{1/2}} \quad (4)$$

Here,  $\eta \in (0, 1]$  is the occupancy of the quadrupoles in the lattice and  $\bar{r}_x = (1/L_p) \int_0^{L_p} ds r_x$ . Equation (4) shows that envelope flutter in a quadrupole channel depends strongly on  $\sigma_0$  and weakly on  $\eta$  (max  $\eta$  variation is  $\sim 13\%$ ).

For a particle evolving both inside and outside of the elliptical beam envelope, Eq. (2) can be expressed as

$$x'' + \kappa_x x = \frac{2QF_x}{(r_x + r_y)r_x} x, \quad (5)$$

with an analogous equation for the  $y$ -plane. Here,  $F_j$  are form factors satisfying  $F_j = 1$  inside the beam ( $x^2/r_x^2 + y^2/r_y^2 \leq 1$ ) and  $F_x = (r_x + r_y)\frac{r_x}{x}\text{Re}[\underline{S}]$  and  $F_y = -(r_x + r_y)\frac{r_y}{y}\text{Im}[\underline{S}]$  outside the beam ( $x^2/r_x^2 + y^2/r_y^2 > 1$ ).  $\underline{S}$  is a complex variable defined as  $\underline{S} \equiv \frac{\underline{z}}{(r_x^2 - r_y^2)^{1/2}} [1 - \sqrt{1 - \frac{r_x^2 - r_y^2}{\underline{z}^2}}]$ , where  $\underline{z} = x + iy$  and  $i = \sqrt{-1}$ .

The particle equations of motion (5) are integrated numerically from initial conditions. Diagnostics include particle trajectories, single particle emittances defined by  $\epsilon_x = \sqrt{(x/r_x)^2 + (xr'_x - x'r_x)^2/\varepsilon_x^2}$  ( $\epsilon_x = 1$  at the core distribution edge), stroboscopic Poincare phase space plots, and particle oscillation wavelengths calculated from Fourier transforms of orbits.

### CORE-PARTICLE SIMULATIONS

To clearly illustrate the resonance, we launch particles along the  $x$ - and  $y$ -axes of the elliptical beam in specified regions outside the beam edge (e.g.,  $x = [1.1, 1.2]r_x$ ) with zero incoherent angle spreads (e.g.,  $x' = r'_x x/r_x$ ). Fig. 3 illustrates  $x-x'$  Poincare phase-spaces for particles launched with  $[1.1, 1.2]r_x$  for fixed  $\sigma_0$  and two values of  $\sigma/\sigma_0$ : (a) a high value (weak space-charge) well within the stable region of Fig. 1, and (b) a low value (strong space charge) in the unstable region. The Poincare strobe is one lattice period. Scaled coordinates  $x/r_x$  and  $(x'r_x - xr'_x)/\varepsilon_x$  are plotted to remove envelope flutter. The extent of the core is plotted. Extrapolations of the range of initial launch conditions are indicated based on the annular elliptical region formed if the initial particle conditions evolved with constant single-particle emittances. For the stable case, particles diving in and out of the matched envelope remain close to the initial launch range and indicate a weak, high-order resonance. For the unstable case, numerous high-order resonances near the core become stronger and overlap causing the region immediately outside the core to break up into a stochastic sea that touches the core.

A large, 4-lobe bounding resonance (KAM surface) persists that ultimately limits the achievable amplitude. Frequency diagnostics verify the phase advance of particles locked in the limiting resonance are  $90^\circ$  per period – showing that the 4th harmonic of the orbit of a particle moving inside and outside the elliptical beam envelope is resonant with lattice oscillations. The phase advance of particles moving outside the envelope is strongly amplitude dependent ranging from  $\sigma$  for amplitudes at the core boundary to  $\sigma_0$  for very large amplitudes. Strong space charge ( $\sigma/\sigma_0 \ll 1$ ) and large matched envelope oscillations (large  $\sigma_0$ ) provide a strong pump at the lattice frequency. Harmonics of particles orbits near the core can strongly resonate with the lattice resulting in overlapping resonances and a strong chaotic transition allowing particles near the core to rapidly evolve to large amplitudes.

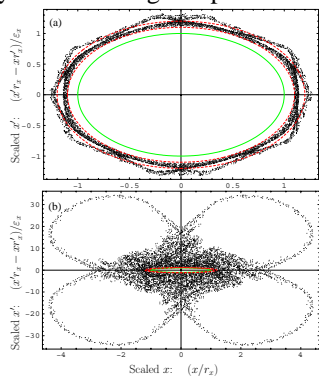


Figure 3: (Color) Core-particle Poincaré phase-spaces for  $\sigma_0 = 100^\circ$ ,  $\sigma/\sigma_0 = 0.67$  (a), and  $\sigma/\sigma_0 = 0.1$  (b). ( $L_p = 0.5$  m,  $\eta = 0.5$ ,  $\varepsilon = 50$  mm-mr) Core = Green, Launch Range = Red

A new stability criteria is defined to estimate where such resonance effects can impact transport. At fixed  $\sigma/\sigma_0$  we defined the stability boundary to be at the first value of  $\sigma_0$  when approached from the stable region where particles launched in a group [1.05, 1.10] times the matched radius increase in amplitude to 1.5 times the matched radius. Boundary points obtained are plotted in Fig. 1 and roughly track the experimental stability boundary. Results are relatively insensitive to the choice in initial group radius and amplitude increase factor. This halo induced mechanism for transport degradation is consistent with increasing sensitivity to the beam distribution and edge perturbations as the threshold region is approached but is not too pessimistic and inconsistent with experiment as previous estimates[5].

Resonance structures persist when particles have finite angular momentum (not launched on-axis). Single particle emittance growths of  $\sim 50$  are possible for particles entering the resonance, making it plausible that the beam phase-space can be significantly distorted and statistical emittance growth large if significant numbers of near-edge particles join the resonance. Diagnostics show that particles entering the resonance rapidly grow in amplitude over a relatively small number of lattice periods – consistent with simulations. The model assumption of a uniform density elliptical beam core is likely a good for small  $\sigma/\sigma_0$  due to Debye screening and phase-mixing of perturbations. Because no periodic, nonuniform density equilibria are known and

core perturbations are observed in PIC simulations to collectively evolve and disperse leaving smaller residual fluctuations and a rounded beam edge, the uniform core model likely gives a good approximation to the average impulse a halo particle experiences traveling through the oscillating core. If the edge of the beam distribution is not sharp, as is expected to for finite  $\sigma/\sigma_0$ , a significant population of edge particles may enter the resonance.

## CONCLUSIONS

A core-particle model was developed to analyze transport limits of beams with high space-charge intensity propagating in periodic focusing channels. This model was applied to analyze previously unexplained transport limits for space-charge dominated beams in periodic quadrupole transport channels that have been experimentally observed for  $\sigma_0 > 85^\circ$ . It was shown that near-edge particles oscillating both inside and outside the matched beam envelope experience nonlinear forces that drive a strong resonance chain that can pump near-edge particle orbits to large amplitude. This resonance halo is distinct from envelope mismatch driven halo because the driving oscillation is the fast flutter of the matched beam envelope. The matched envelope flutter becomes larger with increasing  $\sigma_0$ , providing a strong pump. Lack of edge self-consistency in real beams makes it plausible that many near-edge particles that can move sufficiently outside the beam core to partake in the resonance. Then large distortions in the beam phase-space and statistical emittances measures can result – consistent with observations from PIC simulations. Stability thresholds based on this resonance criteria are in rough agreement with experimental measurements.

Work is ongoing to further clarify the processes described. Core-particle model predictions are being checked with PIC simulations. The core-particle model is also being applied to periodic solenoidal focusing (in the Larmor frame). Preliminary results indicate analogous resonance effect limits are more benign due to smaller envelope flutter with weak-focusing solenoids reducing the driving term. Envelope mismatch effects are also included in the core-particle model and are being explored. Mismatch introduces additional frequencies and increases envelope excursions – possibly reducing the region on stable transport. Edge induced transport limits also likely apply to lattice transition sections (i.e., matching sections) where the beam is more strongly focused to reduce transverse envelope size. Such transitions are equivalent to high local phase advance and can result in loss of beam edge control.

## ACKNOWLEDGMENTS

B. Bukh and J. Barnard helped develop parts of the core-particle model. D. Grote aided the WARP simulations. J. Barnard, I. Haber, E. Lee, and P. Seidl provided useful discussions.

## REFERENCES

- [1] M.G. Tiefenback, *Space-Charge Limits on the Transport of Ion Beams*, LBL-22465 (1986).
- [2] S.M. Lund and B. Bukh, PRSTAB **7** 024801 (2004).
- [3] M. Reiser, *Charged Particle Beams*, (Wiley, 1994).
- [4] D.P. Grote, et al., Nuc. Instr. Meth. A **415** 428 (1998).
- [5] J.-M. Lagniel, Nuc. Instr. Meth. A, **345** 405 (1994).